An Optimal Energy Hub Management Integrated EVs and RES Based on Three-Stage Model Considering Various Uncertainties

ELHAM MOKARAMIAN[1], **HOSSEIN SHAYEGHI**[1], (Senior Member, IEEE), **FARZAD SEDAGHATI**[1], **AMIN SAFARI**[2], **AND HASSAN HAES ALHELOU**[3], (Senior Member, IEEE)

[1]Energy Management Research Center, University of Mohaghegh Ardabili, Ardabil 56199-11367, Iran
[2]Department of Electrical Engineering, Azarbaijan Shahid Madani University, Tabriz 53751-71379, Iran
[3]Department of Electrical Power Engineering, Faculty of Mechanical and Electrical Engineering, Tishreen University, Latakia 2230, Syria

Corresponding author: Hossein Shayeghi (hshayeghi@gmail.com)

ABSTRACT In order to make significant progress in the operation of power systems and minimizing cost and air pollution, multi-carrier energy systems based on the economic and emission problem have been proposed by implementing various solutions and using different sources. In this study, an energy hub (EH) system includes a wind turbine (WT), photovoltaic (PV), and EVs that are exchanged energy with energy and reserve market considering energy, thermal, and gas demand response program is proposed. But these units due to uncertain behavior create a big problem in balancing between the demand and generated energy. Thus, the uncertainty of WT, PV, load, and electricity market price are modeled with Mont-Carlo method. Besides that, all parameters of the EVs with uncertainty behavior are modeled using a new method that classified EVs based on the capacity of the battery and other features. This method is employed a stochastic optimization approach to simplify the uncertainty modeling for increasing the system reliability. Hence, two objective functions, namely economic cost, and environmental cost are considered. Finally, a three-step strategy is introduced to solve the multi-objective problem as a single objective function. Finally, EH management performance is investigated by implementing the proposed method and elements.

INDEX TERMS Demand response program, electric vehicle, energy hub, renewable energy sources, uncertainty.

NOMENCLATURES

EH	Energy hub.
CHP	Combined heat and power.
DRP	Demand response program.
GDRP	Gas demand response program.
EDRP	Electric demand response program.
TDRP	Thermal demand response program.
ESS	Energy storage system.
GAMS	General algebraic modeling system.
RES	Renewable energy storage.
TDRP	Thermal demand response program.
TSS	Thermal storage system.
UP	Upstream grid.
WT	Wind turbine.
PV	Photovoltaic.

Indices

t	Time index.
n	The number of scenarios.
e	Economic index.
m	Emission index.

Parameters

$V_{co}, V_{ci} \& V_R$	Cut off, cut in, and rated speed.
$v(t)$	Wind speed.
$g_{\min}^{grid} \& g_{\max}^{grid}$	Min and max capacity of gas grid.
$\alpha_e^{\min} \& \alpha_e^{\max}$	Min and max capacity of ESS.
$\alpha_h^{\min} \& \alpha_h^{\max}$	Min and max capacity of TSS.
$\eta^{C/L}$	Efficiency of fc.
g_t^l	Gas demand in residential area.

$a_1, a_2,$ b_1, b_2, c, d	Cost coefficient of CHP unit [\$/kwh].
$P_x \mid X \in \{A, B, D, F, G, H, I\}$	Power of corner points in CHP unit in operation zones [kwh].
$H_x \mid X \in \{A, B, D, F, G, H, I\}$	Heat of corner points in CHP unit in operation zones [kwh].
$\bar{M}_x \mid X \in \{A, B, D, F, G, H, I\}$	Max coefficients of Big-M method [kwh].
$M_x \mid X \in \{A, B, D, F, G, H, I\}$	Min coefficients of Big-M approach [kwh].
$LPF^{up,e}, LPF^{dn,e}$	Up and down level of electricity load coefficient.
$LPF^{up,t}, LPF^{dn,t}$	Up and down level of electricity load coefficient.
$LPF^{up,g}, LPF^{dn,g}$	Increased and decreased gas load coefficient.
$\varsigma_e^{ch} \& \varsigma_e^{dis}$	Electricity storage Charge and discharge efficiency.
$\varsigma_h^{ch} \& \varsigma_h^{dis}$	Thermal storage Charge and discharge efficiency.
$\varsigma_{EV}^{ch} \& \varsigma_{EV}^{dis}$	Charge and discharge efficiency of evs.
$P_c^{boiler} \& P_c^{CHP}$	Nominal capacity of boiler & CHP.
P_c^{RM}	Nominal capacity of reserve market.
κ^{FC}	Production price of FC.
κ_t^e	Price of supplied power via upstream grid.
κ_t^{gas}	Natural gas price.
κ^{WT}	Generated power cost of WT.
κ^{PV}	Generated power cost of PV.
κ^{EDRP}	Electricity demand response price.
κ^{TDRP}	Thermal demand response price.
κ^{GDRP}	Gas demand response price.
κ^{TSS}	Cost of generated thermal by TSS.
κ^{ESS}	Cost of generated energy by ESS.
κ^{S}	Cost of generated energy by evs.
$P_{j,0}$	Initial power of EV.
$CO_2^{bo}, SO_2^{bo}, NO_2^{bo}$	Emission coefficient of thermal produced by boiler.
$CO_2^{grid}, SO_2^{grid}, NO_2^{grid}$	Emission coefficient of bought energy by upstream network.
$CO_2^{rl}, SO_2^{rl} NO_2^{rl}$	Emission coefficient of produced electricity by residential area.
$CO_2^{rl}, SO_2^{rl} NO_2^{rl}$	Emission coefficient of bought energy by reserve market.
$CO_2^{chp}, SO_2^{chp}, NO_2^{chp}$	Emission coefficient of CHP unit.
φ	Shape parameter.
ϑ	Scale parameter.
ω, ψ	Shape parameter of Beta Distribution.
σ, τ	Expectation and standard deviation of load.
ς_e^{RM}	Reserve market efficiency.
ς_{gh}^{CHP}	Gas to heat transformer efficiency of CHP.
ς_e^{CHP}	Gas to electricity transformer efficiency of CHP.
ς_{ge}^{boiler}	Gas exchange to heat efficiency of the boiler.
ρ^{CHP}	CHP obtainability.
ρ^{grid}	Upper network obtainability.
ρ^{wind}	WT obtainability.
ρ^{RM}	Reserve market obtainability.
ς_e^{grid}	Transformer efficiency.
ς_e^{wind}	Converter of wind to electricity efficiency.
ς_e^{pv}	Converter of PV to electricity efficiency.
ς_e^{FC}	Converter of FC to electricity efficiency.
$D_{IL}^{thermal}$	Heat demand.
D_{IL}^{EL}	Electricity demand.
Variable	
p_t^{fc}	Generated power by FC.
p_t^e	Imported power from upstream grid.
p_t^{RM}	Imported power from reserve market.
H_t^{bo}	Thermal generated by boiler.
p_t^{wi}	Produced power by WT.

P_t^{PV}	Produced power by PV.
P_t^{FC}	Produced power by FC.
p_t^{CHP}	Electrical power generated by CHP.
H_t^{CHP}	Heat generated by CHP.
$p_t^{ch,e} \& p_t^{dis,e}$	Charge & discharge electricity of ESS.
$p_t^{ch,t} \& p_t^{dis,t}$	Charge & discharge heat of TSS.
$P_{n,t}^{ch}, P_{j,t}^{dis}$	Charge and discharge energy of evs.
p_t^{GAS}	Imported gas from gas network.
p_j^{dem}	Needed power to charge batteries.
$\cos t_{j,t}^{\deg}$	The degradation cost.
$P_t^{up,e}, P_t^{dn,e}$	Increased and deceased electrical load level.
$P_t^{up,t}, P_t^{dn,t}$	Increased and deceased thermal load level.
$P_t^{up,g}, P_t^{dn,g}$	Increased and deceased gas load level.
$f(\upsilon)$	Weibull distribution function.
$f(\theta)$	Weibull distribution function.
$f(x)$	Normal PDF function.
of_{EM}	Total pollution emissions.
g_t^{bo}	Gas consumption of boiler.
obj_i	I_th objective function.
$C_t^{st,e}$	Obtainability energy of electricity storage.
$C_t^{st,h}$	Obtainability energy of heat storage.
$P_{j,f}$	Final battery power.
$P_t^{EL,DR}$	Load of electricity in the presence of DRP.
$P_t^{T,DR}$	Load of thermal in the presence of DRP.
$P_t^{G,DR}$	Load of gas in the presence of DRP.
$P_t^{loss,e}, P_t^{loss,t}$	Losses of energy in ESS and TSS.
p_t^{fc}	Generated power by FC.
p_t^e	Imported power from upstream grid.
p_t^{RM}	Imported power from reserve market.
H_t^{bo}	Thermal produced through boiler.
p_t^{wi}	Produced power by WT.
P_t^{PV}	Produced power by PV.
P_t^{FC}	Produced power by FC.
p_t^{CHP}	Electrical power generated by CHP.
H_t^{CHP}	Heat generated by CHP.

Binary variables

$I_t^{ch,t} \& I_t^{dis,t}$	Charge/ discharge of TSS.
$I_t^{ch,e} \& I_t^{dis,e}$	Charge/ discharge of ESS.
$I_t^{up,e} \& I_t^{dn,e}$	Up and down level of electrical load.
$I_t^{up,t} \& I_t^{dn,t}$	Up and down level of thermal load.
$I_t^{up,g} \& I_t^{dn,g}$	Up and down level of gas load.
I_t^{CHP}	Active and disactivate mode of CHP.
Z_t^1, Z_t^2, Z_t^3	zone activity.

I. INTRODUCTION

A. MOTIVATION

In recent years, in the power system structure, a multi-carrier power system has been implemented instead of the single entity generating [1], [2]. On the other hand, increasing the emission pollution problem due to the use of fossil fuels is one of the serious reasons [3]. Therefore, energy hubs are supposed to play a critical role in the future for solving power system problems [4]. RESs such as PV and wind farms generate clean and unlimited energy [5], and the use of renewable energy is an effective way to promote energy transformation in the energy hub [6]. Today, the use of electric vehicles is increasing due to reducing air pollution and exploitation as consumers and producers (as a battery) [7]. EVs are also profitable for car owners, in addition to the economic and environmental benefits of the power system [8]. Therefore, integrating EVs and energy hubs is a good choice for minimizing operation costs and air pollution. Renewable resources have uncertain behaviors due to climate change, which has a significant impact on the performance and reliability of the EH. On the other hand, EVs include uncertainty behaviors [9]. The most suitable operation of the EH will be obtained using a suitable optimization method and integrating the energy market with the reserve market [10] considering uncertainties in the presence of EVs.

B. LITERATURE REVIEW

Different studies of assessing and analyzing EHs abilities due to many advantages such as economy minimization, emission pollution mitigation, high flexibility, market infrastructure, and energy management in various sections of power systems have been done [2], [11], [12]. EH is made from two parts as an input and output, which contain multi carriers in the input section and multi demands in the output section. Employing renewable resources, suitable converters, energy storages, and redundant connection between EH input and output, supply of demand, reliability, and energy management are enhanced, the operation cost and emission pollution are minimized [13]. Implementing a good framework of EH and an appropriate scheduling program is essential to obtain the best results for EH operation. Alessandra Parisio *et al.* proposed a robust optimization method of EH operations [14]. Also, multi carriers' input, stored and distributed in the EH construction is implemented to supply energy demands. However, renewable sources are a good option for input in the EH framework.

In [15], EH as a combined energy system containing renewable energy resources was proposed considering demand response programs to supply electrical, cooling, and heating demands. But, the stochastic nature in the production of the RESRs has not been considered. In [16], a new

mathematical method for analyzing the integrated EH with a deregulated market was reported. This method is based on a mathematic program with an equilibrium constraints model to investigate the strategic performances of a profit-driven EH in both the heating and electricity markets. Since the economic issue is important in EH performance, at the same rate, the pollution emission is important, too. So, Lu *et al.* in [17], an optimal load program model for a community EH represented. Both EDRP and TDRP to minimize the total cost of the energy hub, including system economic and environmental costs were considered. One of the most effective methods to improve the performance of EH and optimize the operation cost and emission pollution is using an appropriate energy storage system. In [18], and EH management mechanism was introduced by employing two new energy storages are called ice storage conditioner (ISC) and solar-powered compressed air energy storage to minimize operation and emission pollution costs considering combined CHP, photovoltaic, and wind turbine. The other important factor, which has the most effect on EH performance is using a robust scheduling method. Shams *et al.* [19] suggested a min-max min robust method for the short-term scheduling of microgrids integrated with the natural gas network to model the uncertainty of WT generation, electrical, and thermal loads introduced. The proposed model was solved and linearized using the column-and-constraint generation process that divides the framework into a master problem and a sub-problem. It should be better if the improved EH structure behind a suitable scheduling method was analyzed simultaneously. In [20], novel energy storage integrated with an energy hub in an industrial park was proposed and a bi-level optimization scheduling method was introduced to analyze the optimal bidding and programing in the daily market. The main aim of this method is to minimize the day-ahead operation cost.

Since renewable sources are subject to weather conditions, their output power is not constant and has uncertainty. Therefore, it is essential to study the causes of uncertainty with appropriate methods. In [21], an MINLP method for the optimal scheduling of the energy hub was modeled in the presence of uncertainty factors. In addition, the effect of implementing DRPs, determine the size of the energy hub, and implementing a complete energy flow of loads are introduced.

Using the risk-averse method is a good option for modeling the uncertainty of the energy hub to increase reliability. A novel look-ahead risk-constrained based on the look-ahead scheduling technique in the daily market of the energy hub was proposed to reduce the total cost of the energy hub in the presence of DRP in [22]. Mokaramian *et al.* [23], analyzed the performance of the energy hub using a multi-objective function as environmental, economic, load deviation, and risk level objective functions conditional value at risk and second-order stochastic dominance. Also, a new storage model as PHESS has been utilized in EH to optimal energy management considering DRP for water, gas, electricity, and thermal.

In [24], a spatiotemporal association of wind speed, solar irradiation, and price responsive loads in the presence of cooperative and non-cooperative modes of energy hubs using a game-theoretic method is proposed, which has participation by the energy market. In addition, mathematical scheduling with equilibrium restraints was applied to solve the highly competitive behavior of the energy hubs in this market in the presence of system losses. Stochastic operation of energy hub in the uncertain environment and using downside risk restrictions was suggested to minimize the risk-in-cost versus risk control parameter in the heating market with heat DRP in [25]. In [26], a multi-objective method was represented to optimize the operation cost and risk-averse in the energy hub. The conditional value at risk method was implemented to control the harmful effects of the uncertainties.

In [27], a multi-agent system is introduced to model the operation of an EH with electric vehicles and modeled various penetration rates and charging patterns of an electric vehicle. A complete random dispatch algorithm was integrated into a smart charging strategy to obtain the maximum capacity and potential of the vehicle to the grid. XinhuiLu *et al.* [28] presented a novel structure of optimal load dispatch model for a community EH in the presence of thermal and electrical demand response programs. In this model, the gas boiler, CHP unit, PV array, heat storage unit, WT, the random admission of large-scale electric vehicles was considered, and using the Monte- Carlo approach, the uncertainty of EVs is simulated. Also, a robust optimization method was proposed to simulate the price uncertainty. To improve the environmental and economic aspect of the energy hub, a multi-objective optimization method in the presence of compressed air energy storage was integrated with a battery energy storage system in [29]. Also, in the structure of residential EH, a plug-in electric vehicle-based demand response program, renewable energy generation units, thermal energy storage, solar heat collectors, and hot water storage was used. Finally, the load demand uncertainty of EVs is modeled using their corresponding coming–exit time, miles of daily moved, and type of vehicle. The optimal Pareto front of the multi-objective issue was achieved by the ε-constrained approach for different robustness alterations.

Regarding the reviewed literature in EH, some of the drawbacks have seemed that should be improved as follow:

• In some studies, renewable sources, fuel cells, and EVs as energy storage have not been used to improve environmental and economic issues.

• Different DRP for water, gas, thermal, and electrical loads have not been considered.

• The impact of all parameters of EVs uncertainties on the operation of the energy hub has not been esteemed.

• Uncertainty of renewable sources, load uncertainty, market price, and EVs have not been considered, simultaneously.

C. CONTRIBUTION
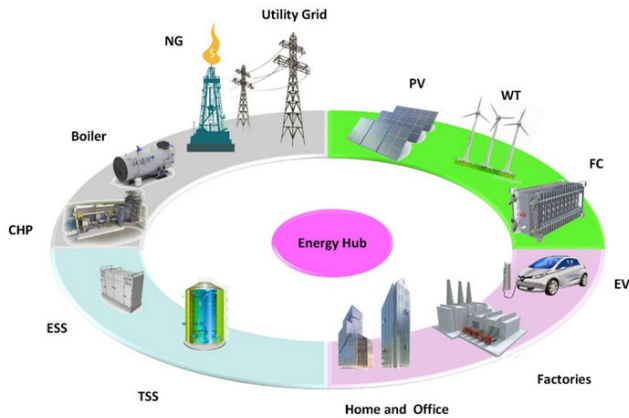In this study, two objectives are considered to optimize the total cost of EH performance as emission pollution and

FIGURE 1. Structure of the proposed EH.

FIGURE 2. CHP unit's heat and power operation zones.

operation cost. The proposed model of EH includes a CHP, boiler, WT, PV, Fuel cell, ESS, HSS, and EV considering the uncertainty of WT, PV, load, price market, and EVs as shown in Fig. 1. In addition, a demand response program is implemented for gas, heat, and electricity demand. All uncertainty factors of EVs as starting and stopping time of charging/discharging period, the overall battery capacity, initial energy, and their number, are not yet addressed for an EH or a collector that uses these resources integrated with renewables to contribute to different electricity markets. So, in this study, we introduce a novel method to implement the storage capacity of EVs as energy storage in EH structure in the day-ahead market. Here, three factors of EVs uncertainties are considered contains EVs capacity uncertainty, coming and leaving time, the amount of energy left in the battery when it becomes obtainable, and their total number.

Finally, the fundamental contributions of this study are mentioned as follow:
- Participating EH with energy and reserve markets
- Integrating the EVs with day-ahead and reserve markets
- Proposing a new method to model all uncertainty parameters of EVs.
- Considering demand response programs for gas, electricity, and thermal loads
- Solving the multi-objective problem using a novel three-stage solution algorithm.

II. ENERGY HUB MODELING
This study presents an EH including different energy carriers with the ability to convert, storing and transferring. The energy hub as shown in Fig. 1 is including utility grid, natural gas network, fuel cell, and renewable sources (wind turbine, PV) in the input section that integrated with ESS and TSS as a storage system, CHP, and boiler in converter section to supply load demand of gas, electricity, heat, and EVs that operate as a mobile storage. The main aim of this study is to minimize operating costs and emission pollution problems. Also, the uncertainty of RES, load market, price of the energy market, and three factors of EVs uncertainties i.e.: EVs capacity uncertainty, coming and leaving time, and their total number are modeled using the Mont-Carlo method.
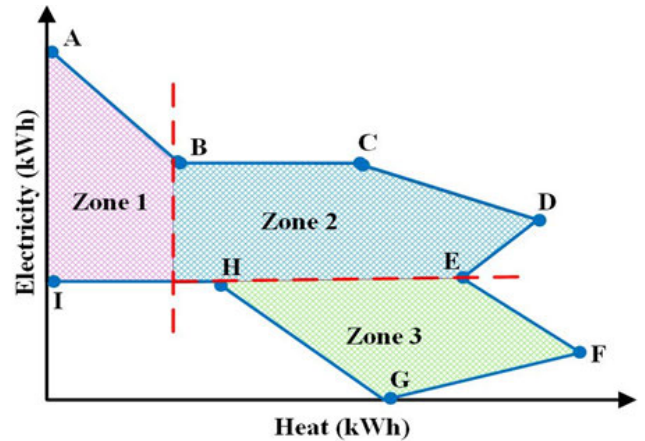
Noted that in this study, EH is assumed as a small city. Electricity and natural gas as input carriers are considered to supply the load demand. Wind turbines and PV can produce electrical energy to use by the consumer. The EVs can operate as bilateral equipment and in the charging mode, is assumed as a consumer, and in discharging mode, the extra power is saved and flow to the EH to use via consumer, in this mode the EVs work as energy storage. The CHP unit in the EH framework is fed from natural gas and produces heat and electrical energy simultaneously. In addition, the auxiliary boiler feeds the natural gas and generates heat to the heating line.

The CHP unit has an important role in EH performance because this unit involved three carriers of EH as natural gas, heat, and electricity. In this study, the CHP unit works in quadratic mode and contains three operational zones, which are shown in Fig. 2.

The relation between the heat and power in CHP operation as shown in Fig. 2, is a non-convex operation zone. When the thermal is produced by the CHP unit, the amount of power generation is limited and conversely. In order to simplify the optimal operation of the CHP unit, the non-convex zone is divided into triple zones which are shown by Zone 1, 2, and 3. Convexness is made by counting three binary variables for the CHP. These zones are convex, and any point on any line in each zone is related to that zone [30].

A. OBJECTIVE FUNCTIONS
The main aims of this study are divided into two parts. The first aim is to minimize total operation cost and the second aim is to optimize the emission pollution cost of the EH in the day-ahead market.

B. ECONOMIC OBJECTIVE FUNCTION
The economic objective function includes two terms to optimize the total cost of the EH as follow [23]:

$$OF_{op} = \sum_{t=1}^{n} Cost_{EH} + \sum_{t=1}^{n} Cost_{RM}^{P} \qquad (1)$$

The first term denotes the operation cost of the EH, and the second term represents the reserve market cost. The energy hub system contains RESs, boiler, CHP unit, thermal and electrical energy storage, and EVs. Demand response program is considered for all types of load demand including gas, thermal and electric demand with a specified cost. So, the operation cost of EH is presented as follow:

$$Cost_{EH} = Cost_{OC}^{up} + Cost_{OC}^{DRP} + Cost_{OC}^{SS} \\ + Cost_{oc}^{RES} + Cost_{OC}^{CHP} + Cost_{OC}^{B} + Cost^{EV} \quad (2)$$

The energy hub system purchase energy from the upstream grid of electric and gas station, which is calculated as follow:

$$Cost_{oc}^{up} = \kappa_t^e P_t^e + \kappa^{Gas} p_t^{Gas} \quad (3)$$

In order to manage energy usage in peak load duration by shifting the energy consumption to low periods, DRP is implemented in the energy hub to cost-minimizing. The main effect of the demand response program is based on the balance between energy consumption and production in each period. Electrical, thermal and gas demand program are expressed as follow:

$$Cost_{OC}^{DRP} = Cost_{OC}^{EDRP} + Cost_{OC}^{TDRP} + Cost_{OC}^{GDRP} \\ = \kappa^{EDRP}(p_t^{UP,E} + p_t^{DN,E}) + \kappa^{TDRP}(p_t^{UP,T} + p_t^{DN,T}) \\ + \kappa^{GDRP}(p_t^{UP,G} + p_t^{DN,G}) \quad (4)$$

Also, the operation cost of the storage system is made from two-part including the electric storage system and thermal storage system as follows.

$$Cost_{OC}^{SS} = Cost_{OC}^{ESS} + Cost_{OC}^{TSS} = \kappa_s^{ESS}(p_E^{ch} + p_E^{dis}) \\ + \kappa_s^{TSS}(p_T^{ch} + p_T^{dis}) \quad (5)$$

The operational cost of the renewable sources is equal to the set of operation costs of the WT, PV, and an FC that is a function of output power.

$$Cost_{OP}^{RES} = \kappa^{WT} p_t^{WT} + \kappa^{PV} p_t^{PV} + \kappa^{FC} p_t^{FC} \quad (6)$$

The operation cost of the CHP unit is a quadratic function of the generated power and heat and given by.

$$Cost_{CHP} = \begin{pmatrix} a_1.\left(p_t^{CHP}\right)^2 + a_2.p_t^{CHP} + b_1.\left(H_t^{CHP}\right)^2 \\ + b_2.H_t^{CHP} + c.p_t^{CHP} H_t^{CHP} + d.I_t^{CHP} \end{pmatrix} \quad (7)$$

The operation cost of the boiler is a function of output power and can be defined as follow:

$$Cost_{boiler} = \kappa_t^{gas} H_t^{bo} \quad (8)$$

In order to provide a suitable economic program for electric vehicles, the objective function is defined based on the amount of charging/discharging energy of electric vehicles. The required energy for charging EVs is provided by EH, P_j^{dem}, with the specific cost, and at the same time when EVs have been used as an energy storage system at time t with specific degradation cost.

which is calculated as follow:

$$Cost_{EV} = \sum_J (P_j^{dem} k^s) - \sum_j \cos t_{j,t}^{deg} \quad (9)$$

The second term of Eq. (1) is the cost of purchasing energy from the reserve market and is formulated by Eq. (10).

$$Cost_{RM}^P(t, e) = \kappa_t^{RM} P_t^{RM} \quad (10)$$

C. ENVIRONMENTAL OBJECTIVE FUNCTION

The environmental issue of the energy hub is critical. So, the emission pollution cost of the three most effective gases (CO_2, NO_2, and SO_2) which are generated through EH equipment is considered in the objective function. The emission cost of EH is produced by the upstream grid, boiler, CHP unit, and consumed residential gas [25].

$$OF_2 = Min(C_{em}) = EM_{grid} + EM_{CHP} + EM_{bo} \\ + EM_{rl} + EM_{RM} \\ = p_t^e(CO_2^{grid} + SO_2^{grid} + NO_2^{grid}) \\ + p_t^{CHP}(CO_2^{CHP} + SO_2^{CHP} + NO_2^{CHP}) \\ + p_t^{bo}(CO_2^{bo} + SO_2^{bo} + NO_2^{bo}) \\ + p_t^{rl}(CO_2^{rl} + SO_2^{rl} + NO_2^{rl}) \\ + p_{RM}^e(CO_2^{grid} + SO_2^{grid} + NO_2^{grid}) \quad (11)$$

D. LIMITATION OF THE EH OPERATION
1) LIMITATION OF ELECTRICAL DR PROGRAM
The equal and unequal limitations of electrical DRP are as follow:

$$P_t^{EL,DR} = P_t^{el} + P_t^{up,e} - P_t^{dn} \quad (12)$$

$$\begin{cases} 0 \le P_t^{up,e} \le LPF^{up,e} P_t^l I_t^{up,e} \\ 0 \le P_t^{dn,e} \le LPF^{dn,e} P_t^l I_t^{dn,e} \end{cases} \quad (13)$$

$$I_t^{up,e} + I_t^{dn,e} \le 1 \quad (14)$$

$$\sum_t^H P_t^{up,e} = \sum_t^H P_t^{dn,e} \quad (15)$$

The constraint of up and low load levels of the EH is formulated by Eq. (13). The increasing and decreasing load level cannot be done at the same time which is modeled in Eq. (14). The EH must save the overall electricity consumption constant in the forecast cycle, which is restricted by Eq. (15).

2) LIMITATION OF THERMAL DR PROGRAM
The equal and unequal limitations of thermal DRP are as follow:

$$P_t^{TL,DR} = P_t^{TL} + P_t^{up,T} - P_t^{dn,T} \quad (16)$$

$$\begin{cases} 0 \le P_t^{up,T} \le LPF^{up,T} P_t^{lT} I_t^{up,T} \\ 0 \le P_t^{dn,T} \le LPF^{dn,T} P_t^{lT} I_t^{dn,T} \end{cases} \quad (17)$$

$$I_t^{up,T} + I_t^{dn,T} \le 1 \quad (18)$$

$$\sum_t^H P_t^{up,T} = \sum_t^H P_t^{dn,T} \quad (19)$$

Similar to the EDRP, Eq. (17) formulates the limitation of increased/decreased load of the energy hub. The restraint to cope with the increasing/decreasing of the thermal load level at the same time is modeled by Eq. (18). The amount of increasing/decreasing thermal load should be equal which is formulated by Eq. (19).

3) LIMITATION OF GAS DR PROGRAM
The equal and unequal constraints of gas DRP are as follow:

$$P_t^{GL,DR} = P_t^{GL} + P_t^{up,G} - P_t^{dn,G} \tag{20}$$

$$\begin{cases} 0 \le P_t^{up,G} \le LPF^{up,G} P_t^{lG} I_t^{up,G} \\ 0 \le P_t^{dn,G} \le LPF^{dn,G} P_t^{lG} I_t^{dn,G} \end{cases} \tag{21}$$

$$I_t^{up,G} + I_t^{dn,G} \le 1 \tag{22}$$

$$\sum_t^H P_t^{up,G} = \sum_t^H P_t^{dn,G} \tag{23}$$

The exact definitions of the previous sections apply to GDRP.

4) LIMITATION OF ESS
Another important factor in the EH framework is to save the extra produced power by units. So, ESS is used to deal with energy losses. The mathematical formulation and limitation of ESS are stated as [20]. The electrical energy balance restraint of the ESS unit is given by Eq. (24). The saved electrical energy by the ESS unit should be restricted in a confident range, which is given by Eq. (25). The maximum charging/discharging powers of the ESS unit are restricted by Eqs. (26) and (27), respectively. The electrical loss of ESS is given by Eq. (28). Eq. (29) guarantees that ESS cannot be charged and discharged at the same time.

$$C_t^{st,e} = C_{t-1}^{st,e} + (p_t^{ch,e} \varsigma_e^{ch}) - (p_t^{dis,e}/\varsigma_e^{ch}) - p_t^{loss,e} \tag{24}$$

$$\alpha_{min}^e C_c^{st,e} \le C_t^{st,e} \le \alpha_{max}^e C_c^{st,e} \tag{25}$$

$$\frac{\alpha_{min}^e C_c^{st,e} I_t^{ch,e}}{\varsigma_{ch}^e} \le p_t^{ch,e} \le \frac{\alpha_{max}^e C_c^{st,e} I_t^{ch,e}}{\varsigma_{ch}^e} \tag{26}$$

$$\alpha_{min}^e C_c^{st,e} I_t^{ch,e} \varsigma_{dis}^e \le p_t^{dis,e} \le \alpha_{max}^e C_c^{st,e} I_t^{dis,e} \varsigma_{dis}^e \tag{27}$$

$$p_t^{loss,e} = \alpha_{loss}^e C_t^{st,e} \tag{28}$$

$$I_t^{ch,E} + I_t^{dis,E} \le 1 \tag{29}$$

5) LIMITATION OF TSS
Thermal demand in the energy hub is at a high level, so it is necessary to save the extra produced power by units. Thus, TSS is used to deal with energy losses. The equal and unequal constraints of TSS are [20].

$$C_t^{st,tss} = C_{t-1}^{st,t} + (p_t^{ch,t} \varsigma_e^{ch}) - (p_t^{dis,t}/\varsigma_e^{ch}) - p_t^{loss,t} \tag{30}$$

$$\alpha_{min}^t C_c^{st,t} \le C_t^{st,t} \le \alpha_{max}^t C_c^{st,t} \tag{31}$$

$$\frac{\alpha_{min}^t C_c^{st,t} I_t^{ch,t}}{\varsigma_{ch}^t} \le p_t^{ch} \le \frac{\alpha_{max}^t C_c^{st,t} I_t^{ch,t}}{\varsigma_{ch}^t} \tag{32}$$

$$\alpha_{min}^{tt} C_c^{st,t} I_t^{ch,t} \varsigma_{dis}^t \le p_t^{dis,t} \le \alpha_{max}^t C_c^{st,t} I_t^{dis,t} \varsigma_{dis}^t \tag{33}$$

$$p_t^{loss,t} = \alpha_{loss}^t C_t^{st,t} \tag{34}$$

$$I_t^{ch,t} + I_t^{dis,t} \le 1 \tag{35}$$

The exact definitions of the previous sections are implemented to TSS.

6) ENERGY BALANCE CONSTRAINT
The produced or bought energy from the upstream grid in all-time should be equal to the demand for energy. So, electrical, thermal, and gas balance constraint are expressed as follow, respectively.

$$\begin{aligned} D_{IL}^{electrical} + p_t^{UP} - p_t^{DN} \\ = [\rho^{grid} p_t^e \varsigma_e^{grid}] + [p_t^{dis,e} - p_t^{ch,e}] \\ + [\rho^{RM} P_t^{RM} \varsigma_e^{RM}] + [\rho^{chp} p_t^{chp} \varsigma_e^{chp}] \\ + [\rho^{wind} p_t^{wind} \varsigma_e^{wind}] \\ + [\rho^{pv} p_t^{pv} \varsigma_e^{pv}] + [\rho^{FC} p_t^{FC} \varsigma_e^{FC}] \\ + \sum_j e_{n,t}^{dis} \varsigma_{EV}^{dis} - \sum_j e_{n,t}^{ch} \frac{1}{\varsigma_{EV}^{ch}} \end{aligned} \tag{36}$$

$$D_{IL}^{thremal}(t) = \varsigma_{gh}^{bo} H_t^{bo} + [\rho^{CHP} H_t^{CHP} \varsigma_{gh}^{CHP}] + (P_t^{dis} - P_t^{ch}) \tag{37}$$

$$g_t^{grid} = g_t^{boiler} + g_t^{CHP} + g_t^l \tag{38}$$

A nominal rate is definitely for purchasing power from the upstream grid that should supply transformers nominal capacity constraint and total bought gas limitation from the gas grid.

$$\rho^{grid} \times P_t^e \le P_C^T \tag{39}$$

$$g_{min}^{grid} \le g_t^{grid} \le g_{max}^{grid} \tag{40}$$

7) RESERVE MARKET CONSTRAINT
Total buying power from the reserve market should be equal to the nominal capacity.

$$P_t^{RM} \le P_C^{RM} \tag{41}$$

8) MODEL OF BOILER AND CHP
The boiler is fed by natural gas and it is necessary to meet the upper and lower level of natural gas input constraints [30].

$$\varsigma_{ge}^{boiler} g_t^{boiler} \le P_c^{boiler} \tag{42}$$

As stated in the previous sections, the operation of CHP is a nonlinear behavior with the triple-zone of electricity and thermal production. The generated heat through the CHP unit is frequently proportional to its electric generation. In addition, heat operation constraints will be guaranteed if the electrical performance constraint is confirmed [31]. Limitations associated with the CHP unit with three operational areas as shown
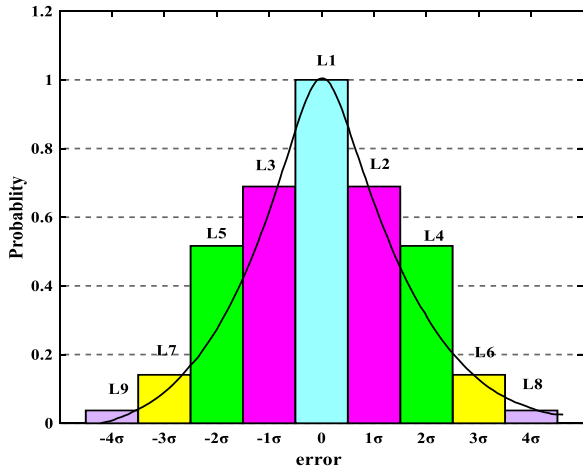
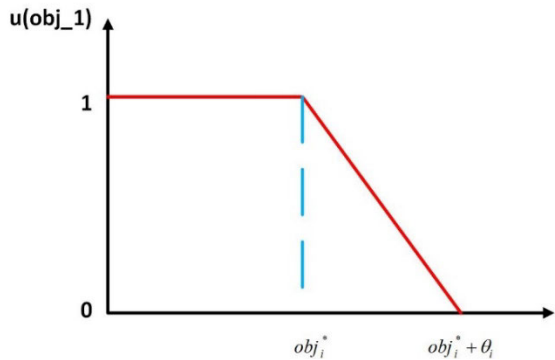**FIGURE 3.** Discretization of a continuous distribution into several levels [34].

FIGURE 4. The reducing half gradient membership function.

in Fig. 4 are formulated as follows:

$$
\begin{cases}
P_t^{CHP} - P_B - \dfrac{P_B - P_A}{H_B - H_A}[H_t^{CHP} - H_B] \\
\qquad \leq [1 - Z_t^1].\underset{AB}{\bar{M}} \qquad \forall t \\[4pt]
P_t^{CHP} - P_C - \dfrac{P_C - P_D}{H_C - H_D}[H_t^{CHP} - H_C] \\
\qquad \leq [1 - Z_t^2].\underset{CD}{\bar{M}} \qquad \forall t \\[4pt]
P_t^{CHP} - P_D - \dfrac{P_D - P_E}{H_D - H_E}[H_t^{CHP} - H_D] \\
\qquad \geq [1 - Z_t^2].\underset{DE}{\bar{M}} \qquad \forall t \\[4pt]
P_t^{CHP} - P_E - \dfrac{P_E - P_F}{H_E - H_F}[H_t^{CHP} - H_E] \\
\qquad \leq [1 - Z_t^3].\underset{EF}{\bar{M}} \qquad \forall t \\[4pt]
P_t^{CHP} - P_F - \dfrac{P_F - P_G}{H_F - H_G}[H_t^{CHP} - H_F] \\
\qquad \geq [1 - Z_t^3].\underset{FG}{\bar{M}} \qquad \forall t \\[4pt]
P_t^{CHP} - P_G - \dfrac{P_G - P_H}{H_G - H_H}[H_t^{CHP} - H_G] \\
\qquad \geq [1 - Z_t^3].\underset{GH}{\bar{M}} \qquad \forall t
\end{cases}
\tag{43}
$$

$$
\begin{cases}
H_t^{CHP} - H_B \leq \left|1 - Z_t^1\right|.M_{E1} & \forall t \\[4pt]
H_t^{CHP} - H_B \geq \left|1 - Z_t^2\right|.M_{E21} & \forall t \\[4pt]
P_t^{CHP} - P_H \geq \left|1 - Z_t^1\right|.M_{H1} & \forall t \\[4pt]
P_t^{CHP} - P_E \geq \left|1 - Z_t^1\right|.M_{E22} & \forall t \\[4pt]
P_t^{CHP} - P_E \leq \left|1 - Z_t^3\right|.M_{E3} & \forall t
\end{cases}
\tag{44}
$$

$$
Z_t^1 + Z_t^2 + Z_t^3 = I_t^{CHP}
\tag{45}
$$

$$
\begin{cases}
P_t^{CHP} \leq P_A.I_t^{CHP} \\
H_t^{CHP} \leq H_F.I_t^{CHP}
\end{cases}
\tag{46}
$$

Using the big-M method, the upper and lower range are defined via $\bar{M}$ and M, that represent inactive at the predicted time [30].

9) SOURCES MODEL

- Wind turbine

The produced power by the wind turbine is proportional to wind speed and is given by [23].

$$
P_{wind} =
\begin{cases}
0 & v \leq V_{ci} \\
P_{wind}^{rate}\left(\dfrac{v - V_{ci}}{V_R - V_{ci}}\right) & V_{ci} \leq v \leq V_R \\
P_{wind}^{rate} & V_R \leq v \leq V_{co} \\
0 & V_{co} \leq v
\end{cases}
\tag{47}
$$

- Photovoltaic

The imported power by the PV system is proportional to the solar irradiance as follow [32]:

$$
P_t^{pv} = \eta_t^{pv} A^{pv} G_t \quad \forall t \in T
\tag{48}
$$

- Fuel Cell

The power made through the FC in each period $t \in \{1, 2, \cdots, NT\}$, H_{2t}^{FC}, which is proportional with the hydrogen feeding in peck period is expressed as [32]:

$$
H_{2t}^{EL} = (P_t^{EL} - P_t^{FC}/\eta^{C/l})\eta^{EL} \quad \forall t = 1
\tag{49}
$$

$$
H_{2t}^{EL} = H_{2_{t-1}}^{FC}(P_t^{EL} - P_t^{FC}/\eta^{C/l})\eta^{EL} \quad \forall t > 1
\tag{50}
$$

Several constraints related to fuel cell performance are:

$$
\begin{cases}
P_t^{EL} \leq \bar{P}^{EL} y_t^{EL} & \forall t \in T \\
P_t^{FC} \leq \bar{P}^{FC} y_t^{FC} & \forall t \in T \\
y_t^{EL} + y_t^{FC} \leq 1 & \forall t \in T
\end{cases}
\tag{51}
$$

10) EVs CONSTRAINTS

The constraints of EVs participation in EH operation and their real-life restrictions are defined as:

$$
P_{j,f} = P_j^{dem} + P_{j,0} \quad n \in N
\tag{52}
$$

Eq. (52) represents the final battery power of the EV when the plug-in time is ended, which is equal to the total of the demanded energy through j_th EV and the initial power of the EV battery [33]. The plug-in time of EV is in the interval of

[$t_{b,j}$, $t_{e,j}$], and the demanded energy of the EV can be defined by the difference between needed energy for charging the battery and used energy by EVs in the day ahead and reserve markets.

$$P_{j,t+1}^{dem} = P_{j,t}^{dem} + \sum_{j=t_{b,j}}^{t_{e,j}} p_{j,t}^{ch} \zeta_{EV,ch} - p_{j,t}^{DA,dis}/\zeta_{EV,ch}$$
$$- p_{j,t}^{RES,dis} \quad n \in N \quad (53)$$

For charging/discharging an EV battery, a certain bound is considered equal to the battery conditions and existing equipment minus the charging and discharging facilities. Also, the charging and discharging operation cannot be done at the same time.

$$\begin{cases} p_{j,t}^{dis,DA} + p_{j,t}^{dis,RES} \leq DR_n(1 - u_{n,t}^{ch}) & n \in N \\ p_{j,t}^{ch,DA} \leq CR_n u_{n,t}^{ch} & n \in N \end{cases} \quad (54)$$

The amount of energy in EVs batteries at the arrival and departure time is formulated as follow:

$$P_{j,t}^{dem} = P_{j,t}^{arr} \quad \forall j, t = Arrival\ time$$
$$P_{j,t}^{dem} = P_{j,t}^{dep} \quad \forall j, t = Departure\ time \quad (55)$$

The power of the j_th EV at time t is related to three factors including the initial state of the battery, charging/discharging power of the EV at the same time. The starting and stopping time of the charging and discharging of the battery is also formulated as follow:

$$\begin{cases} p_{j,t}^{EV} = p_{j,t-1}^{EV} + p_{j,t}^{ch}\zeta_{ch} - p_{j,t}^{DA,dis} - p_{j,t}^{RES,dis} \\ \quad \forall t \in [t_{b,j}, t_{e,j}], \ n \in N \\ p_{j,t}^{EV} = P_{j,0} + p_{j,t}^{ch}\zeta_{ch} - p_{j,t}^{DA,dis} - p_{j,t}^{RES,dis} \quad t = t_{b,j}, \\ \quad \forall n \in N \\ p_{j,t}^{EV} = P_{j,f} \ t = t_{e,j}, \\ \quad \forall n \in N \end{cases} \quad (56)$$

E. STOCHASTIC SIMULATION FOR MODELING THE UNCERTAINTY

Some of the energy carriers' parameters in the EH have random and vague behavior. Therefore, it is hard to predict this parameter's behavior. Finding an appropriate method to forecast these parameters' function with high reliability is significant.

The output power of WT and PV is related to climate changes, and their forecasted power includes uncertainty. So, using a stochastic model can try to achieve the most exact model. Moreover, the price of the energy market and load demand are affected by consumer demand and climate behavior. Like WT and PV, it is essential to implement an effective stochastic method to model the uncertainty of these parameters.

Finally, for the first time in the EH performance, all of the EV parameters that have uncertain behavior consist of coming and leaving time, the energy remaining in the battery

when it becomes available, and the number of EH is considered.

A scenario-based stochastic model is implemented to model the uncertainty behavior of all parameters.

F. SCENARIO GENERATION

In this model, a PDF of each parameter is used and shown in Fig. 3. Scenarios of the PDF curve are divided into seven levels. Each is of PDF contains a probability rate. It should be noted that the center of the fourth scenario is the same predicted value.

1) SOLAR IRRADIANCE UNCERTAINTY

Since the output power of the solar is a function of the solar irradiance and weather variation. Beta PDF is used to model the uncertainty of solar irradiance. Beta PDF is a function of two parameters as ω and ψ [35]:

$$f(\theta) = \begin{cases} \frac{\Gamma(\omega)\Gamma(\psi)}{\Gamma(\omega) + \Gamma(\psi)}\theta^{\omega-1}(1-\theta)^{\psi-1}, \\ \quad 0 \leq \theta \leq 1, \ \omega \geq 0, \ \psi \geq 0 \\ 0, \\ \quad otherwise \end{cases} \quad (57)$$

where the ψ and ω variables are computed as follow:

$$\psi = (1 - \mu)(\frac{u \times (1 - \mu)}{\sigma^2} - 1) \quad (58)$$

$$\omega = \mu[\frac{\mu(1 - \mu)}{\sigma^2} - 1] \quad (59)$$

2) WIND SPEED UNCERTAINTY

Similar to the solar operation, wind speed is a function of weather changes. So, the Weibull distribution function is implemented to model the wind speed uncertainty [36].

$$f(\upsilon) = \frac{\varphi}{\vartheta}(\frac{\upsilon}{\vartheta})^{\varphi-1}e^{-(\frac{\upsilon}{c})^{\varphi}} \quad (60)$$

3) UNCERTAINTY OF MARKET PRICE AND LOAD

Since the exact value of consumer demands and energy market price is not definite. A normal PDF function is used to model the load and market price uncertainty.

$$f(x) = \frac{1}{\partial\sqrt{2\pi}}e^{-(\frac{(x-\tau)^2}{2\partial^2})} \quad (61)$$

4) EVs UNCERTAINTY

In this study, EVs operate in a dual state as both consumer and energy storage. The EV has three factors of uncertainty behavior. The saved energy in the battery at the start, their availability, and needed energy is unclear when the battery is in the charge or discharge state.

Similar to another uncertainty parameter, EH can detect the charging state and behavior of EVs in the parking lots.

In order to simplify the uncertainty modeling of the EVs, like the [37], EVs are categorized into different types. Each type of electric vehicle has its specifications. These futures include the obtainability time, initial state of the battery, and

capacity of the battery. In this method, 1000 different EVs are classified into 100 types. So, in addition to the small number of EVs and uncertainty parameters are studied, the EVs' parameters are linked together, characterizing them causes the chance to analyze the uncertainty in a more straightforward and improved way.

Each type of EV in the EH has grouped base on the {Eu,0, [tb,u, te,u], Emax,u} by assuming that u ∈U.

Implementing this method is caused to reduce the sources of the uncertainty parameter to the number of EVs. Here, the number of EVs from each group is assumed as an uncertain parameter.

The uncertainty of the EVs with w scenarios and type u are formulated as follow:

$$n_{w,u} = \hat{n}_u + err_w^{nu} \quad u \in U \tag{62}$$

To model the uncertainty of EVs numbers, the normal distribution method with zero mean and σn as the distribution error is implemented.

G. K-MEANS CLUSTERING METHOD
In this paper, five uncertainty parameters are modeled. The PDF is divided into nine levels, and each level represents various scenarios and errors. In the first step, 1000 scenarios for each parameter are generated with the mentioned method and using the k-means clustering approach the scenario numbers are reduced to 10 scenarios in the MATLAB environment.

H. MULTI-STAGE SOLUTION METHOD
In this study, two functions as economic and emission pollution objectives are considered. A multi-stage solution is proposed that consists of three stages [38].

First stage: payoff table establishment
Second stage: fuzzy linearization
Third stage: Objective weight calculation.

1) PAYOFF TABLE ESTABLISHMENT
The payoff table is implemented to investigate the relationship between the various objective functions. This table is used to calculate the weight coefficients. The stages of the establishment are as follow:

The objective function is chosen as the optimization objective obji (i = 1, 2 . . . , I) where the i_th objective function value is objii and another objective functions values are objik(i, k = 1, 2, . . . , I).

The pay of table is structured as Table.1 based on the obtained value of the objective functions. Then the lower and upper value of the objectives is used for objective weight competition and fuzzy linearization.

The fuzzy linearization and objective value competition are described in the next section.

2) FUZZY LINEARIZATION
In this study, the descending half-line membership function is used to process the objective functions of the minimum oper-

TABLE 1. Payoff table of the multi-objective functions.

Objective functions	Value of the objective function		
	obj$_{j1}$	obj$_{j2}$	$\cdots$ obj$_{jI}$
obj_1	obj_{11}	obj_{12}	$\cdots obj_{1I}$
obj_2	obj_{21}	obj_{22}	$\cdots obj_{2I}$
$\vdots$			
obj_i	$\vdots$	$\ddots$	$\vdots$
	obj_{i1}	obj_{i2}	$\cdots obj_{II}$

ation cost and the minimum carbon emissions. The specific method is as follows:

$$\rho(obj_i) = \begin{cases} 1, & obj_i \geq obj_i^* \\ \dfrac{obj_i - (obj_i^* + \theta_i)}{\theta_i}, & obj_i^* < obj_i \\ & < obj_i^* + \theta_i \\ 0, & obj_i \leq obj_i^* \end{cases} \tag{63}$$

Eq. (63) represents the half-life reducing half gradient membership function and is utilized to procedure the objective functions of the minimum operation cost, which is shown in Fig. 4.

3) OBJECTIVE WEIGHT CALCULATION
The objective authorization approach is applied to compute the weight coefficients. The pre-processed objective function decision matrix [obj$_{ji}$k]I×I is calculated by Table 1. Then, to compute the weight of the objective function, the entropy weight approach is used by implementing the different degrees of the objective function. So, the weights of any objective could be calculated by the entropy weight approach [39] as:

$$E_i = -\varphi \sum_{j=1}^n n_{ij} \ln(r_{ij}'), \quad i = 1, 2, \ldots, k \tag{64}$$

where $\varphi = 1/\ln(n)$ is the constant represented with the sample number, where Ei ∈ [0, 1]. r'ij meets 0 < r ij' < 1, and $\sum$ r'ij = 1 when rij = 0, rijln(rij) = 0.

• Compute the weights of the objective function obji as follows:

$$d_i = 1 - E_i, \quad i = 1, 2, \ldots, k \tag{65}$$

$$\lambda_i = \frac{d_i}{\sum_{i=1}^i d_i}, \quad i = 1, 2, \ldots, k \tag{66}$$

Based on the weight coefficients of various objective functions, the total single objective function can be formulated as follows:

$$OBJ = \sum_{i=1}^I \lambda_i \mu(obj_i), \tag{67}$$

where, OBJ represents the total single objective function, which can achieve the best acceptable solution for matching all objective functions.
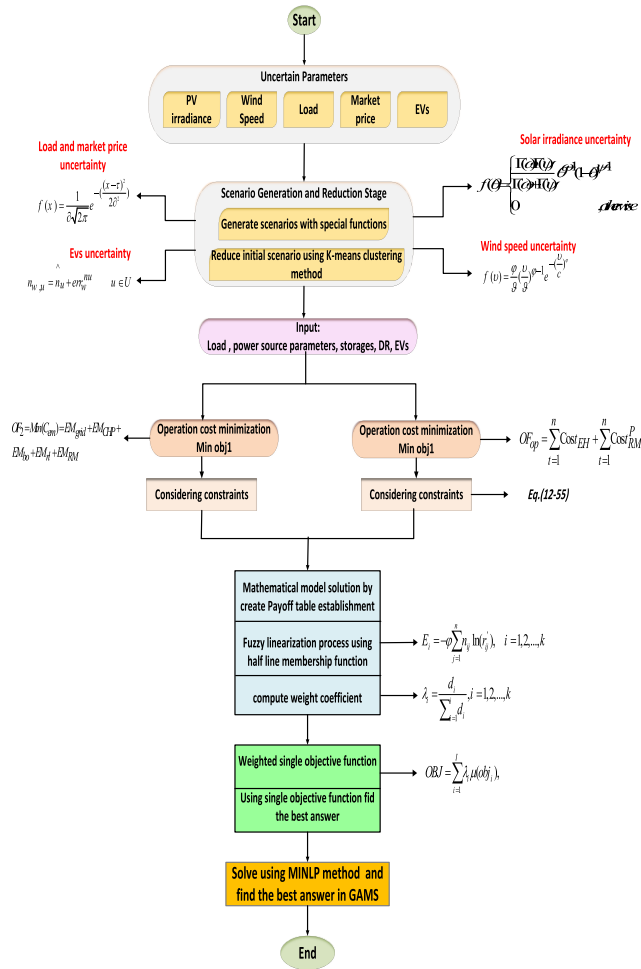
FIGURE 5. The solution steps of the multi-objective functions.

Fig. 5 depicts the flowchart of the proposed solution method to optimize energy management of the EH as a multi-objective problem.

III. NUMERICAL RESULTS AND SIMULATION

In this section, the optimum scheduling of the proposed EH as shown in Fig. 1 are studied in the energy and reserve markets. It includes renewable sources as WT, PV, and fuel cell, storages as ESS and TSS, and EVs in both states of storage and generator.

A. INPUT DATA

In this part, all the essential data for implementing the short-term optimized scheduling of the proposed EH is presented. The main aim of the proposed structure is to minimize the economic and emission pollution costs using participating in the day-ahead energy and reserve markets. All of the needed data are categorized in two sections a real-time data and forecasted data. The needed forecasted data as WT speed, solar irradiance, load demand, market price, and number of EVs based on the real-time data are made using the Mont Carlo approach in 600 scenarios, and the by k-mean cluster-
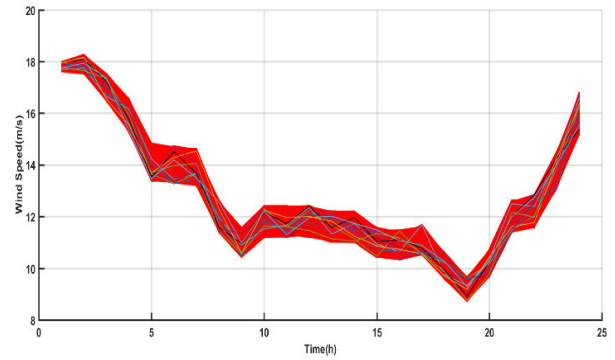
FIGURE 6. Produced and decreased scenarios for wind speed.
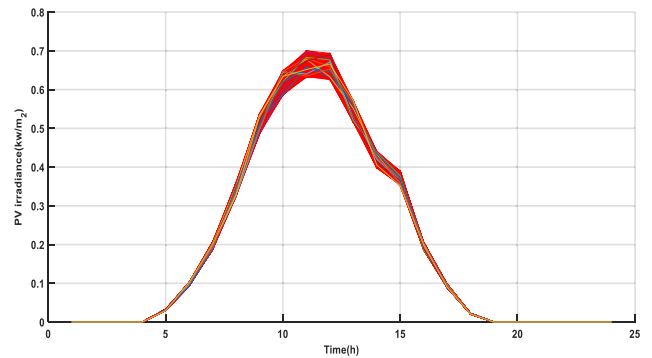
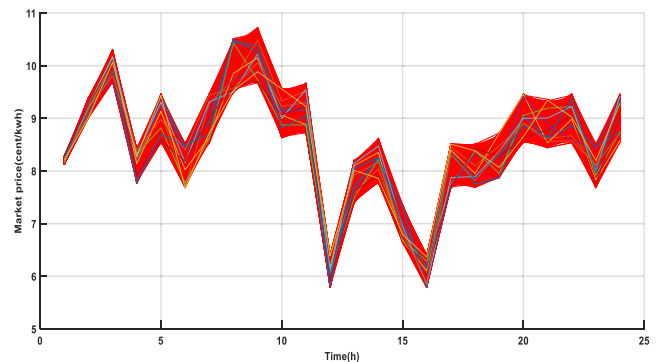**FIGURE 7.** Produced and decreased scenarios for PV irradiance.

FIGURE 8. Produced and decreased scenarios for energy market price.

ing method these data are decreased to ten scenarios. In Fig. 6, wind turbine speed scenarios with the red line, and 10 reduced scenarios with different color is plotted. Similar to the wind turbine, other mentioned uncertainty parameters are shown in Figs.7-9.

The last uncertain parameter is the EVs number of each type of electric vehicle based on the battery capacity in the interval of [5 90] kwh and also charging/discharging enabling which have enhanced all time significantly. Some of the parameters used to classify electric vehicles are analyzed in [40]. The obtained necessary data are integrated with the proposed method of scenario generation. 11 types of popular
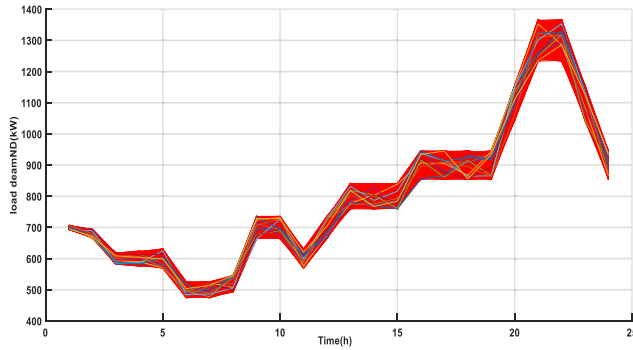
FIGURE 9. Produced and decreased scenarios for electrical load demand.

TABLE 2. Typical EVs in the market regarding their storage capacity [40].

Vehicle brand	Volkswage n Grp	Renault	Hyundai Grp	Tesla	Daimler Grp.	BMW Grp	Groupe PSA	Nissan	Jaguar	Honda	All others
Market share (%)	38.3	16.2	12.0	8.7	8.7	8.0	3.3	2.4	0.6	0.2	1.4
Battery capacity (kWh)	40	24	32	8.5	17	12.3	21	20.4	23.4	27	25

EVs, based on the availability, capacity, and another critical behavior parameter, in the German market with sales statices are introduced in Table 2 [40]. Moreover, their percentage is used as a range in [0 1]. In every iteration, a random number among the 0 and 1 states which type of EVs is chosen. Based on the total capacity of parking lots, the number of each type of EV is produced. The number of different types of EVs for the day-ahead in each scenario, the overall number of EVs in each scenario, and the reduced 10 number scenarios are depicted in Fig. 10.

Fig. 11 shows the energy, gas, and heat demand of the EH (kW). Table 3 lists the essential parameters of TSS, ESS, and WT. The real-time energy demand and reserve market price are exposed in Fig. 12. The data associated with the various units in the energy hub (CHP, boiler, gas, grid, PV, etc.) is given in Table 4. The emission factor of NO2, SO2, and CO2 in each unit of EH in kg/kWh is presented in Table 5. In Fig. 13, the required parameters of the CHP unit are defined. The operation cost of numerous grids and units are given in Table 6.

Finally, the proposed EH model with stochastic constraints has a nonlinear behavior that is modeled using the equivalent MINLP method and is solved with CPLEX in GAMS.

In order to assess the proposed method, three cases are classified as follow:

Case 1: Simple EH without EVs and reserve market
Case 2: Considering the EVs and uncertainty factors
Case3: Considering EH with EVs and reserve market.
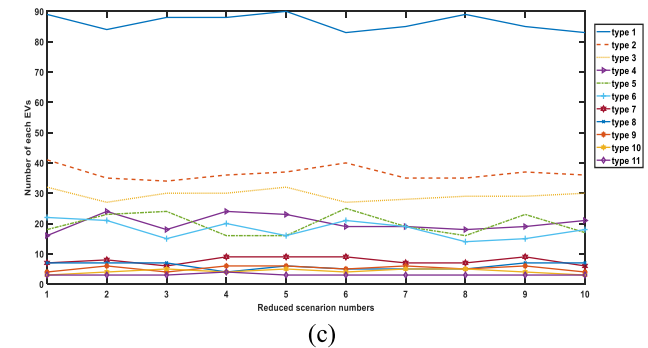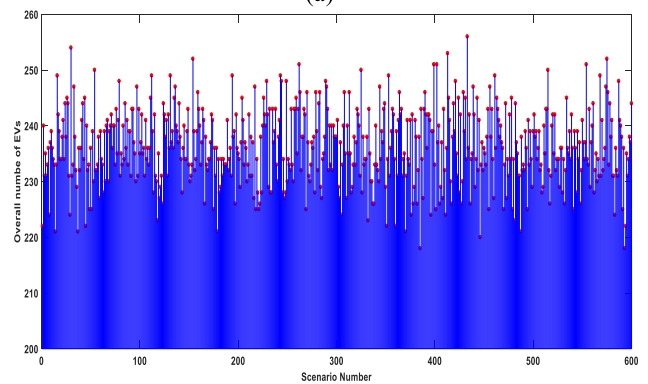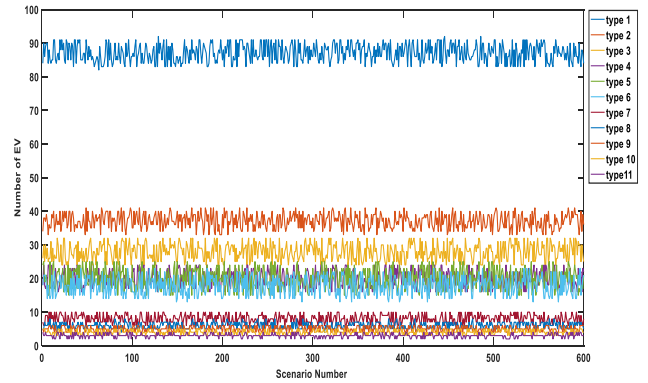

(a)

(b)

(c)

FIGURE 10. (a) The number of different types of EVs for the day-ahead in each scenario (b) Total number of EVs for the day-ahead in each scenario (c) reduced 10 number scenarios of each type of EVs.

TABLE 3. TSS, ESS, and WT parameters.

ESS	Value	TSS	Value	WT	value
α_e^{min}	0.06	α_h^{min}	0.06	ρ^{wind}	0.96
α_e^{max}	0.92	α_h^{max}	0.92	V_r	10 m/s
ς_e^{ch}	92 %	ς_h^{ch}	92 %	V_{ci}	4 m/s
ς_e^{dis}	92 %	ς_h^{dis}	92 %	V_{co}	22 m/s
ψ^{ESS}	180 kW	ψ^{TSS}	250 kW	x, y, z	0.070, 0.010, 0030
α_e^{loss}	0.2	α_T^{loss}	0.2	P_{wind}^{rate}	400 kW

Case 1: In this case, the simple structure of the EH is assumed and both objective functions are minimized using the multi-stage solution method. At first, to investigate the
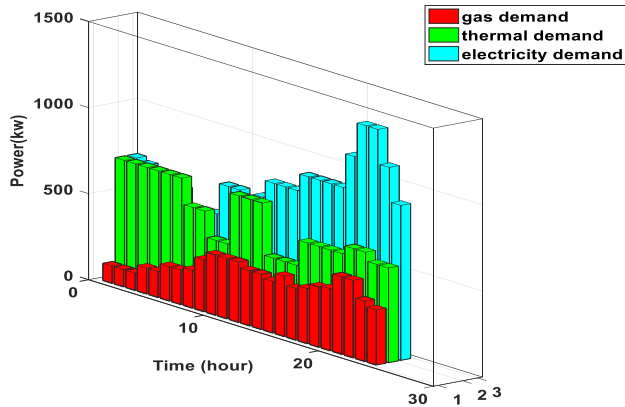
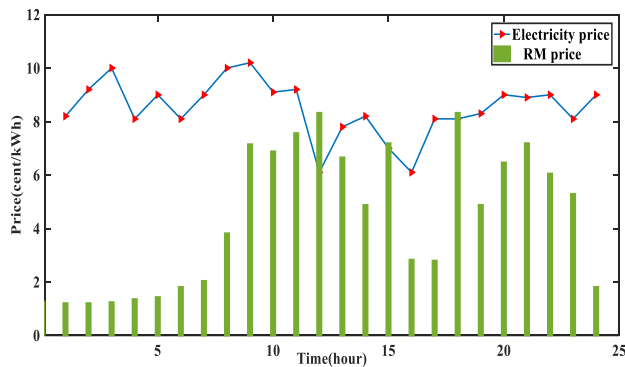**FIGURE 11.** Energy, gas, and heat demand of energy hub.

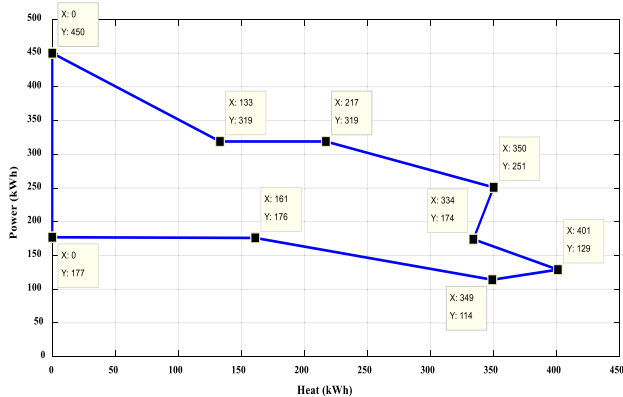**FIGURE 12.** Electricity market and reserve market cost [24].

FIGURE 13. Cartesian diagram of CHP unit output.

TABLE 4. The required data of various units in EH.

Parameter of CHP				Boiler, gas, grid, and PV parameter [20]	
ς_{gh}^{CHP}	45 %	a_2	0.90625	ς_{gh}^{bo}	90 %
ς_{ge}^{chp}	40 %	b_1	0.00188	P_c^{boiler}	700 kW
ρ^{CHP}	0.94 %	b_2	0.2625	g_{max}^{grid}	900-1700 kW
P_c^{CHP}	800 kW	c	0.00188	A^{PV}	400 m²
a_1	0.00216	d	16.56	η_t^{PV}	0.12
Upstream grid parameter [20]				EVs parameter	
ρ^{grid}	0.99			k_s	55 ($/Mwh)
p_{max}^e	1000 kW			Parking-lots capacity	260
p_{min}^e	0 kW			ς_{EVs}^{dis}	0.95
P_C^T	800 kW			ς_{EVs}^{ch}	0.95

TABLE 5. The emission coefficient of EH units.

Units	NO₂ (kg/kWh)	SO₂ (kg/kWh)	CO₂ (kg/kWh)
Boiler	0.000085	0.0000031	0.36
CHP	0.000085	0.0000031	0.36
DG emission	0.000085	0.0000031	0.36
Residential area	0.00070	0.000026	0.355
Grid emission	0.00075	0.00020	0.370

TABLE 6. The operation cost of upstream grid and units.

Parameter	Value (Cent/kWh)	Parameter	Value (Cent/kWh)
ψ_t^{gas}	6	ψ^{DRP}	2
ψ^{wind}	1	ψ^{TSS}	2
ψ^{PV}	1	ψ^{EVs}	10
ψ^{FC}	1	ψ^{ESS}	2

TABLE 7. Compared methods.

Methods	Operation cost ($)	Emission pollution cost ($)
Hybrid method of augmented ε - constraint and fuzzy method [30]	2581.700	10190.837
ε-constraint method [23]	2522.053	11747.201
Multi-stage solution method	2487.808	10089.064

respectively. It is obvious that implementing DRP is caused to reduce both objective functions. The purchasing power from the upstream and gas network are shown in Fig. 14. Also, the output power of renewable sources is shown in Fig. 15.

Case 2: In this case, the EVs are integrated with EH, and the uncertainty factor of solar irradiance, wind speed, market price, load, and EVs are applied. The total number of EVs is equal to 21. The operation cost and emission pollution values are $ 2109.250 and 8139.657 kg, respectively which is decreased about 15.2% and 19.32% rather than case 1, respectively. It is clear that implementing the EVs is caused to reduce both objective functions, as EVs don't produce
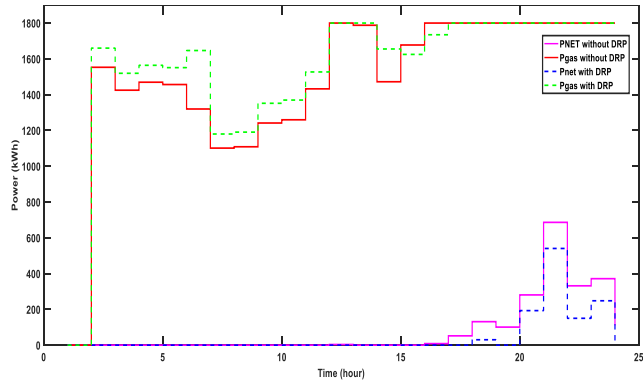
difference between novel multi-stage method and other methods presented in [31], the results are shown in Table 7:

So, applying a new method, in addition to responding quickly and easily, reduces the operation and emission pollution costs. The total operation cost of EH without and with EDRP, TDRP, and GDRP is $2581.700, $2487.808, respectively. Also, the emission pollution of EH without and with EDRP, TDRP, and GDRP are 10190.837kg, 10089.064kg,

FIGURE 14. Imported power from upstream grid and gas network with and without DRP.

FIGURE 15. The output power of WT, PV, and FC.

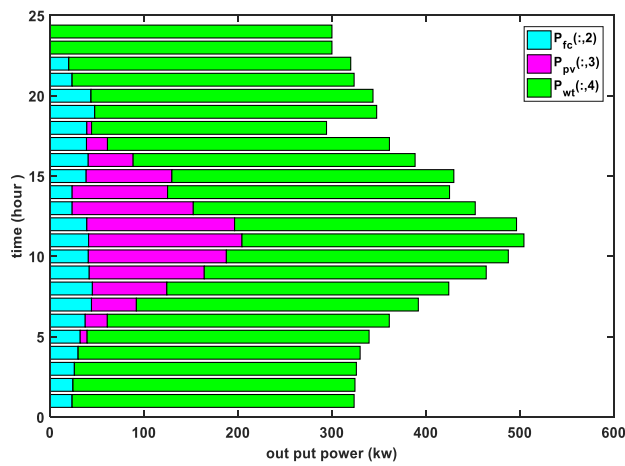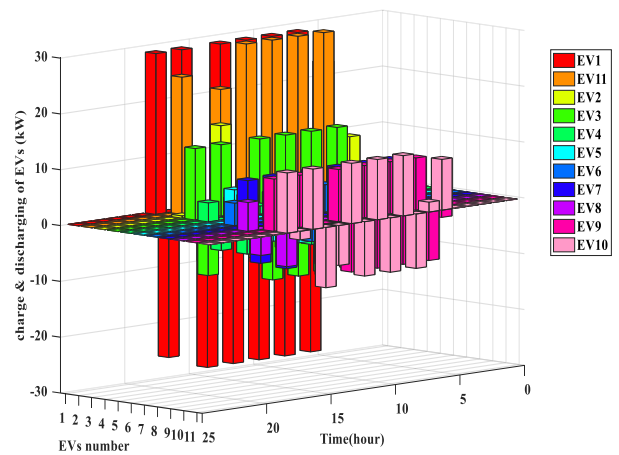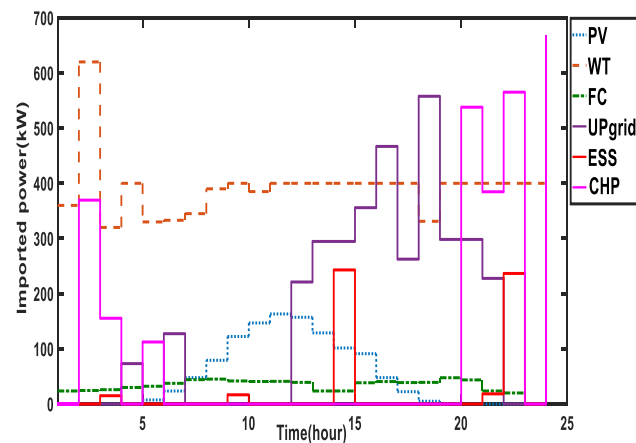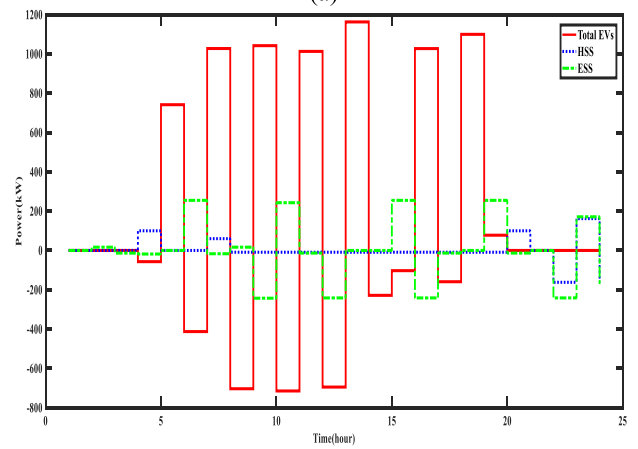**FIGURE 16. Imported power by a different unit.**

**FIGURE 17. Imported power by a different unit.**

(a)

(b)

FIGURE 18. a). charge and discharge level of 11 EVs, (b) Charge and discharge power of total EVs, ESS, and TSS.

emission pollution, this cost is significantly reduced but the most effective of EVs is on the emission pollution issue due these devices do not produce any pollution. In Fig. 16, produced power by different units of EH is shown. Also, the purchased gas from CHP, boiler, and gas network are plotted in Fig. 17. Finally, the charged and discharge power of EVs,

ESS, and TSS is represented in Fig. 18. Most of the required energy for EH is provided by EVs because the emission and cost of EVs are appropriate for the ESS and TSS.

Charge and discharge power of total EVs, ESS, and TSS.
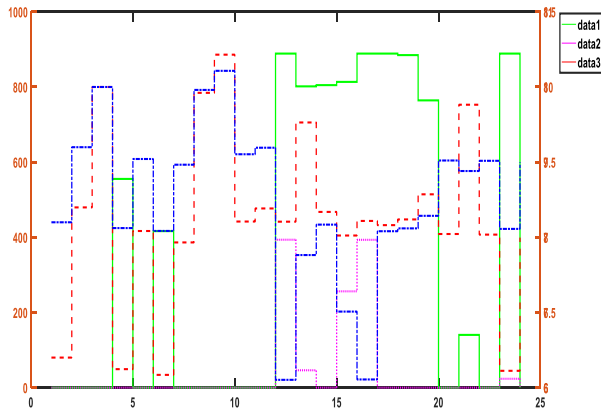
FIGURE 19. Day-ahead forecast the cost of energy and reserve markets, bought energy by the upstream grid and reserve market.

TABLE 8. The best result for three test cases using a multi-stage method.

Case	Operation cost ($)	Emission pollution (kg)
Case 1	2487.808	10089.064
Case 2	2109.250	8139.657
Case 3	1638.577	7642.973

It is clear from Fig.18 that part of the rechargeable energy of electric vehicles is used to supply the demanded energy.

Case 3: Finally, in this case, EH is participating with the reserve market for energy management. In this case, when the load demand is high, EH tries to buy energy from the reserve market at a low price. So, the amount of buying energy from the upstream network with high costs is reduced. In this case, the operation cost and emission pollution value are $1638.577 and 7642.973 kg, respectively. The operation cost of case 3 relative to the case 2 and 1 is decreased about 22.31% and 34.1%. Also, the emission pollution value of case 3 related to case 2 and case 1 is reduced by about 6.1% and 24.2%. Therefore, it can be concluded that the reserve market has a greater impact on operating costs. In Fig. 19, day-ahead forecasting cost of energy and reserve markets bought energy via upstream grid and reserve market is shown. It is clear that applying the reserve market is caused to flat the profile of load.

Finally, the operation costs and emission pollution costs of the 3 cases are listed in Table. 8. As expected, implementing EVs is caused to the reduction of both objective functions relative to case 1, but the second objective is significantly reduced. Finally, participating in the reserve market is a good choice for energy management in peak time and also operation cost minimization.

IV. CONCLUSION

In this study, the short-term optimal scheduling of EH as a small city using a stochastic optimization method was applied with two objective functions in the energy and reserve market. In EH, three storages consisting of TSS, ESS, and EVs in discharging mode, were used. Renewable and nonrenewable resources such as WT, PV, FC, CHP, upstream grid, and natural gas station were considered. The economic operation cost and air pollution problem were considered as a bi-level objective considering EDRP, TDRP, and GDRP, to obtain the EH optimal scheduling in an uncertain situation. The wind speed, solar irradiance, loads, market price, and the number of EVs were assumed as uncertain parameters. The multi-stage solution method was applied to speed up system performance and simplify procedures of the bi-objective optimization problem. One of the main aids of this study is integrating the EVs with the EH considering the three uncertainties of EVs. This three-parameter is converted to one uncertainty parameter which is the number of EVs. Also, due to the uncertain behavior of some elements, implementing appropriate storage is a good option.

Three test cases are defined to analyze the effectiveness of the proposed method with considering reserve market and EVs. Case 1 was considered as a base case of the EH without EVs and reserve market, however, in this case, the effect of applying different DRPs was investigated. In case 2, EVs were integrated with the EH and both modes of consumer and producer are applied. Two objective functions (economic and environmental cost) were decreased by about 5.34% and 3.54%, compared to Case 1, respectively. Finally, the energy hub has traded with the energy and reserve markets for bidding and sailing energy. In this case, the operation and pollution emission costs were decreased compared to Case 2 by about 6.27%, and 8.63%, respectively. It can be concluded that the operation cost and pollution emission of the EH is highly minimized by implementing the proposed three-stage method and reserve market participation in an uncertain environment.

REFERENCES

[1] M. Mohammadi, Y. Noorollahi, B. Mohammadi-Ivatloo, and H. Yousefi, "Energy hub: From a model to a concept—A review," *Renew. Sustain. Energy Rev.*, vol. 80, pp. 1512–1527, Dec. 2017.

[2] X. Zhang, M. Shahidehpour, A. Alabdulwahab, and A. Abusorrah, "Optimal expansion planning of energy hub with multiple energy infrastructures," *IEEE Trans. Smart Grid*, vol. 6, no. 5, pp. 2302–2311, Sep. 2015.

[3] S. Bahramara and H. Golpára, "Robust optimization of micro-grids operation problem in the presence of electric vehicles," *Sustain. Cities Soc.*, vol. 37, pp. 388–395, Feb. 2018.

[4] H. Sadeghi, M. Rashidinejad, M. Moeini-Aghtaie, and A. Abdollahi, "The energy hub: An extensive survey on the state-of-the-art," *Appl. Thermal Eng.*, vol. 161, Oct. 2019, Art. no. 114071.

[5] S. R. Bull, "Renewable energy today and tomorrow," *Proc. IEEE*, vol. 89, no. 8, pp. 1216–1226, Aug. 2001.

[6] M. Murshed, "Can regional trade integration facilitate renewable energy transition to ensure energy sustainability in south Asia?" *Energy Rep.*, vol. 7, pp. 808–821, Nov. 2021.

[7] S. Li, W. Hu, D. Cao, T. Dragičević, Q. Huang, Z. Chen, and F. Blaabjerg, "Electric vehicle charging management based on deep reinforcement learning," *J. Mod. Power Syst. Clean Energy*, pp. 1–12, 2021.

[8] R. Gough, C. Dickerson, P. Rowley, and C. Walsh, "Vehicle-to-grid feasibility: A techno-economic analysis of EV-based energy storage," *Appl. Energy*, vol. 192, pp. 12–23, Apr. 2017.

[9] W. Infante, J. Ma, X. Han, and A. Liebman, "Optimal recourse strategy for battery swapping stations considering electric vehicle uncertainty," *IEEE Trans. Intell. Transp. Syst.*, vol. 21, no. 4, pp. 1369–1379, Apr. 2020.

[10] E. Mokaramian, H. Shayeghi, F. Sedaghati, A. Safari, and H. H. Alhelou, "A CVaR-robust-based multi-objective optimization model for energy hub considering uncertainty and E-fuel energy storage in energy and reserve markets," *IEEE Access*, vol. 9, pp. 109447–109464, 2021.

[11] X. Lu, Z. Liu, L. Ma, L. Wang, K. Zhou, and N. Feng, "A robust optimization approach for optimal load dispatch of a community energy hub," *Appl. Energy*, vol. 259, Oct. 2020, Art. no. 11419.

[12] F. Jamalzadeh, A. H. Mirzahosseini, F. Faghihi, and M. Panahi, "Optimal operation of energy hub system using hybrid stochastic-interval optimization approach," *Sustain. Cities Soc.*, vol. 54, Mar. 2020, Art. no. 101998.

[13] R. Li, W. Wei, S. Mei, Q. Hu, and Q. Wu, "Participation of an energy hub in electricity and heat distribution markets: An MPEC approach," *IEEE Trans. Smart Grid*, vol. 10, no. 4, pp. 3641–3653, Jul. 2018.

[14] A. Parisio, C. Del Vecchio, and A. Vaccaro, "A robust optimization approach to energy hub management," *Int. J. Elect. Power Energy Syst.*, vol. 42, no. 1, pp. 98–104, 2012.

[15] B. Faridpak, A. Alahyari, M. Farrokhifar, and H. Momeni, "Toward small scale renewable energy hub-based hybrid fuel stations: Appraising structure and scheduling," *IEEE Trans. Transport. Electrific.*, vol. 6, no. 1, pp. 267–277, Mar. 2020.

[16] V. Davatgaran, M. Saniei, and S. Mortazavi, "Optimal bidding strategy for an energy hub in energy market," *Energy* vol. 148, pp. 482–493, 2018.

[17] X. Lu, Z. Liu, L. Ma, L. Wang, K. Zhou, and N. Feng, "A robust optimization approach for optimal load dispatch of community energy hub," *Appl. Energy*, vol. 259, Feb. 2020, Art. no. 114195.

[18] M. Jalili, M. Sedighizadeh, and A. S. Fini, "Stochastic optimal operation of a microgrid based on energy hub including a solar-powered compressed air energy storage system and an ice storage conditioner," *J. Energy Storage*, vol. 33, Jan. 2021, Art. no. 102089.

[19] M. H. Shams, M. Shahabi, M. MansourLakouraj, M. Shafie-Khah, and J. P. S. Catalão, "Adjustable robust optimization approach for two-stage operation of energy hub-based microgrids," *Energy*, vol. 222, May 2021, Art. no. 119894.

[20] D. Wu, J. Bai, W. Wei, L. Chen, and S. Mei, "Optimal bidding and scheduling of AA-CAES based energy hub considering cascaded consumption of heat," *Energy*, vol. 233, Oct. 2021, Art. no. 121133.

[21] P. Li, Z. Wang, J. Wang, W. Yang, T. Guo, and Y. Yin, "Two-stage optimal operation of integrated energy system considering multiple uncertainties and integrated demand response," *Energy*, vol. 225, Jun. 2021, Art. no. 120256.

[22] X. Xu, W. Hu, W. Liu, Y. Du, R. Huang, Q. Huang, and Z. Chen, "Look-ahead risk-constrained scheduling for an energy hub integrated with renewable energy," *Appl. Energy*, vol. 297, Sep. 2021, Art. no. 117109.

[23] E. Mokaramian, H. Shayeghi, F. Sedaghati, and A. Safari, "Four-objective optimal scheduling of energy hub using a novel energy storage, considering reliability and risk indices," *J. Energy Storage*, vol. 40, Oct. 2021, Art. no. 102731.

[24] A. Heidari and R. C. Bansal, "Probabilistic correlation of renewable energies within energy hubs for cooperative games in integrated energy markets," *Electr. Power Syst. Res.*, vol. 199, Oct. 2021, Art. no. 107397.

[25] M.-W. Tian, A. G. Ebadi, K. Jermsittiparsert, M. Kadyrov, A. Ponomarev, N. Javanshir, and S. Nojavan, "Risk-based stochastic scheduling of energy hub system in the presence of heating network and thermal energy management," *Appl. Thermal Eng.*, vol. 159, Aug. 2019, Art. no. 113825.

[26] M. Roustai, M. Rayati, A. Sheikhi, and A. Ranjbar, "A scenario-based optimization of smart energy hub operation in a stochastic environment using conditional-value-at-risk," *Sustain. Cities Soc.*, vol. 39, pp. 309–316, May 2018.

[27] H. Lin, Y. Liu, Q. Sun, R. Xiong, H. Li, and R. Wennersten, "The impact of electric vehicle penetration and charging patterns on the management of energy hub multi-agent system simulation," *Appl. Energy*, vol. 230, pp. 189–206, Oct. 2018.

[28] X. Lu, Z. Liu, L. Ma, L. Wang, K. Zhou, and N. Feng, "A robust optimization approach for optimal load dispatch of community energy hub," *Appl. Energy*, vol. 259, Feb. 2020, Art. no. 114195.

[29] S. Zeynali, N. Rostami, A. Ahmadian, and A. Elkamel, "Robust multi-objective thermal and electrical energy hub management integrating hybrid battery-compressed air energy storage systems and plug-in-electric-vehicle-based demand response," *J. Energy Storage*, vol. 35, Mar. 2021, Art. no. 102265.

[30] S. M. Nosratabadi, M. Jahandide, and J. M. Guerrero, "Robust scenario-based concept for stochastic energy management of an energy hub contains intelligent parking lot considering convexity principle of CHP nonlinear model with triple operational zones," *Sustain. Cities Soc.*, vol. 68, May 2021, Art. no. 102795.

[31] S. M. Nosratabadi, R. Hemmati, and P. K. Gharaei, "Optimal planning of multi-energy microgrid with different energy storages and demand responsive loads utilizing a technical-economic-environmental programming," *Int. J. Energy Res.*, vol. 45, no. 5, pp. 6985–7017, Apr. 2021.

[32] F. Cingoz, A. Elrayyah, and Y. Sozer, "Optimized resource management for PV–fuel-cell-based microgrids using load characterizations," *IEEE Trans. Ind. Appl.*, vol. 52, no. 2, pp. 1723–1735, Mar. 2016.

[33] H. Rashidizadeh-Kermani, H. Najafi, A. Anvari-Moghaddam, and J. Guerrero, "Optimal decision-making strategy of an electric vehicle aggregator in short-term electricity markets," *Energies*, vol. 11, no. 9, p. 2413, Sep. 2018.

[34] T. Niknam, R. Azizipanah-Abarghooee, and M. R. Narimani, "An efficient scenario-based stochastic programming framework for multi-objective optimal micro-grid operation," *Appl. Energy*, vol. 99, pp. 455–470, Nov. 2012.

[35] G. Gruosso and P. Maffezzoni, "Data-driven uncertainty analysis of distribution networks including photovoltaic generation," *Int. J. Electr. Power Energy Syst.*, vol. 121, Oct. 2020, Art. no. 106043.

[36] S. Sánchez, V. Hidalgo, M. Velasco, and D. Puga, "Parametric study of a horizontal axis wind turbine with similar characteristics to those of the Villonaco wind power plant," *J. Appl. Res. Technol. Eng.*, vol. 2, no. 2, pp. 51–62, 2021.

[37] A. Ashtari, E. Bibeau, S. Shahidinejad, and T. Molinski, "PEV charging profile prediction and analysis based on vehicle usage data," *IEEE Trans. Smart Grid*, vol. 3, no. 1, pp. 341–350, Mar. 2012.

[38] L. Ju, Q. Tan, Y. Lu, Z. Tan, Y. Zhang, and Q. Tan, "A CVaR-robust-based multi-objective optimization model and three-stage solution algorithm for a virtual power plant considering uncertainties and carbon emission allowances," *Int. J. Electr. Power Energy Syst.*, vol. 107, pp. 628–643, May 2019.

[39] L. Ju, Z. Tan, H. Li, Q. Tan, X. Yu, and X. Song, "Multi-objective operation optimization and evaluation model for CCHP and renewable energy-based hybrid energy system driven by distributed energy resources in China," *Energy*, vol. 111, pp. 322–340, 2016.

[40] *Market Share of Electric Vehicles in Germany From 2014 to 2021*. Accessed: Mar. 2021. [Online]. Available: https://www.statista.com/statistics/1166826/electric-vehicles-market-share-germany/

ELHAM MOKARAMIAN received the B.S. and M.Sc. degrees in electrical engineering from the University of Mohaghegh Ardabili (UMA), Ardabil, Iran, in 2013 and 2016, respectively, where she is currently pursuing the Ph.D. degree in electrical engineering. Her major research interests include hub energies, smart grids, renewable energy, and application of artificial intelligence to power systems.

HOSSEIN SHAYEGHI (Senior Member, IEEE) received the Ph.D. degree in electrical engineering from the Iran University of Science and Technology, Tehran, Iran, in 2006. He is currently a Full Professor and the Scientific Director of the Energy Management Research Center, University of Mohaghegh Ardabili, Ardabil, Iran. He has authored and coauthored of 12 book chapters in international publishers and more than 425 articles in international journals and conference proceedings that received in Google Scholar more than 6505 citations with an H-index equal to 40. His research interests include power system control and operation, microgrid and smart grids control and energy management, and FACTs device. He has been included in the Thomson Reuters' list of the top 1% of most-cited technical engineering scientists in 2015–2021 continuously. He is the Editor-in-Chief of *Journal of Operation and Automation in Power Engineering* and *Journal of Energy Management and Technology*.

AMIN SAFARI received the B.Sc. degree in electrical engineering from the University of Tabriz, Tabriz, Iran, in 2007, the M.Sc. degree from the University of Zanjan, in 2009, and the Ph.D. degree from the Iran University of Science and Technology, Iran, in 2013. He is currently an Assistant Professor with the Department of Electrical Engineering, Azarbaijan Shahid Madani University, Tabriz. He has published more than 140 articles in international journals and conference proceedings. His research interests include the application of artificial intelligence and heuristic optimization algorithms to power system design, FACTS device, power system analysis and control, renewable energy, control and management of microgrids, and smart grid. He was selected as a Distinguished Researcher of the Azarbaijan Shahid Madani University, in 2016.

HASSAN HAES ALHELOU (Senior Member, IEEE) is currently a Faculty Member with Tisheen University, Lattakia, Syria. He is included in the 2018 and 2019 Publons list of the top 1% best reviewer and researchers in the field of engineering. He has published more than 100 research articles in the high-quality peer-reviewed journals and international conferences. He has participated in more than 15 industrial projects. His current research interests include power systems, power system dynamics, power system operation and control, dynamic state estimation, frequency control, smart grids, micro grids, demand response, load shedding, and power system protection. He was a recipient of the Outstanding Reviewer Award from *Energy Conversion and Management* journal, in 2016, *ISA Transactions* journal, in 2018, *Applied Energy* journal, in 2019, and many other awards. He was also a recipient of the Best Young Researcher in the Arab Student Forum Creative among 61 researchers from 16 countries at Alexandria University, Egypt, in 2011. He has also performed reviews for high prestigious journals, including the IEEE Transactions on Industrial Informatics, the IEEE Transactions on Industrial Electronics, *Energy Conversion and Management*, *Applied Energy*, and the *International Journal of Electrical Power and Energy Systems*.

FARZAD SEDAGHATI was born in Ardabil, Iran, in 1984. He received the M.S. and Ph.D. degrees in electrical engineering from the University of Tabriz, Tabriz, Iran, in 2010 and 2014, respectively. In 2014, he joined the Faculty of Engineering, Mohaghegh Ardabili University, where he has been an Assistant Professor, since 2014. His current research interests include renewable energies and hub energies.

● ● ●